PREPARATION AND CHARACTERIZATION OF γ-AgI IN SUPERIONIC COMPOSITE GLASSES $(AgI)_x(AgPO_3)_{1-x}$

S. Suminta[1], E. Kartini[2] and T. Sakuma[3]

[1,2] Center for Nuclear Industry Material Technology - (BATAN)
Puspiptek, Serpong 15314, Indonesia
[3] Department of Physics, Faculty of Science
Ibaraki University, Mito 310-8512 Japan

ABSRACT

PREPARATION AND CHARACTERIZATION OF γ-AgI IN SUPERIONIC COMPOSITE GLASSES $(AgI)_x(AgPO_3)_{1-x}$. The γ-AgI phase was stabilized at room temperature in the composites glasses $(AgI)_x(AgPO_3)_{1-x}$ with x = 0.6 and 0.7 via rapid quenching of their molten mixture. The measurement of the crystal structure has been carried out using an X-ray Difractometer at the Physics Departement of Ibaraki University, Japan. The micro strain and crystal size are derived from Hall's equation. The X-ray diffraction pattern shows some Bragg peaks that correspond to the crystalline γ-AgI. By increasing the concentration of AgI, the peak width becomes more narrow and the position shifts to the higher angle. This indicates that the crystalline size and microstrain are increasing. The increase of micro strain (η), and particle size (D) will increase the ionic mobility, thus increasing the ionic conductivity. It is concluded that solidification process on melt AgI into glass matrix $AgPO_3$ not only decreases the micro strain and the particle size, but it also increases the ionic conductivity.

Keyword : Micro strain, Particle size, Composite, and γ-AgI phase

INTRODUCTION

Recently there has been substantial technological development on electronic devices and computer. Due to this reason, the availability of small size power source such as solid state batteries are strongly needed. Some researchers in the field of solid state physics have spent a lot of effort in producing superionic conductor due to its promising applications in batteries and sensor [1]. This material can work at room or higher temperatures. Our research team has been working to contribute in fulfilling the requirements. The works were started by studying one of the components of the batteries i.e. the glass based electrolyte $(AgI)_x(AgPO_3)_{1-x}$, by Kartini et al.[2]. The working temperature of the electrolyte varies with the amount of the doping salt. The glass transition temperatures are in the region of 40 to 230 °C [3] and it depends on the amount of the AgI dopant. It has been found that the higher the amount of the dopant the lower the glass transition temperature. The maximum solubility of AgI dopant in $AgPO_3$ is x = 0.57 [1-4].

Currently, there is increasing demand on developing new solid electrolytes for practical applications such as solid state batteries, smart

windows, fuel cells and sensor devises. Many research efforts have been attempled to fulfill the need through seeking new materials that meet the criteria to be useful as a solid electrolytes. Some of these criteria are follows : high room temperature ionic conductivity, transferensce number close to unity and temperature stability [5,6]. Crystalline AgI and Ag_2S are only unable as practical as ionic conductors only in their high temperature phases well above the room temperature. AgI has three different crystalline phases [2,5]. At room temperature the predominant phase is γ-AgI phase with the zinc-blende face-centered-cubic structure F-4 3 m, though usually some β-AgI is also present with the wurtzite hexagonal structure $P6_3mmc$. β-AgI becomes the more stable phase above 384 K, although coexistence of the phases may still occur. Both phases transform to body-centered-cubic α-AgI at 420 K with an increase of conductivity by three orders of magnitude to 10^{-2} S/cm. α-AgI meets the requirement of having sufficienly high ionic conductivity. The problem is that it is not stable at ambient temperature while most appliances work at ambient temperature.

The α-AgI phase of silver iodide, which is one of the best superionic conductors, only thermodynamically stable above 147^oC. However it was found to be stable at room temperature in a glass matrix by means of rapid quenching of the melt [6]. Sinse then α-AgI has been successfully stabilized at room temperature in a variety of superionic glasses in the systems such as AgI-Ag_2O-MxOy, where M_xO_y is B_2O_3, P_2O_5, GeO_2, V_2O_5, MoO_3, WO_3 by using a rapid quenching procedure [7,8]. The α-AgI composites exhibit extremely high ion coductivities of about 10^{-2} – 10^{-1} S cm^{-1} at room temperature and low activation energies of about 15 kJ mol^{-1} [9]. In the present paper, we present the preparation, microstructure, phase transformation and low temperature behavior of rapidly quenched γ-AgI-Ag_2O-P_2O_5 or $(AgI)_x(AgPO_3)_{1-x}$ (molar ratio Ag_2O/P_2O_5 = 2) composites in which γ-AgI was stabilized at room temperature.

EXPERIMENTAL METHODS

The superionic glass samples $(AgI)_{0.6}(AgPO_3)_{0.4}$ and $(AgI)_{0.7}(AgPO_3)_{0.3}$ were prepared by mixing the appropriate amounts of AgI, $AgNO_3$ and $NH_4H_2PO_4$. The mixture was finely ground and placed into a porcelain crucible and heated gradually up to 600 ^oC within 6 hours. The melt was quenched into liquid nitrogen to achieve rapid quenching. Clear yellowish transparant glasses were obtained for $(AgI)_{0.6}(AgPO_3)_{0.4}$ and $(AgI)_{0.7}(AgPO_3)_{0.3}$, respectively. Step Counting of X-ray diffraction measurements were carried out to check the quality of the superionic glasses. X-ray Difraction measurements were performed for all quenched glasses by using a Shimadzu instrument at the Physics Departement of Ibaraki University, Japan.

RESULTS AND DISCUSSION

The X-ray patterns show several peaks on amorphous background, indicating that the sample have been partially crystallized.
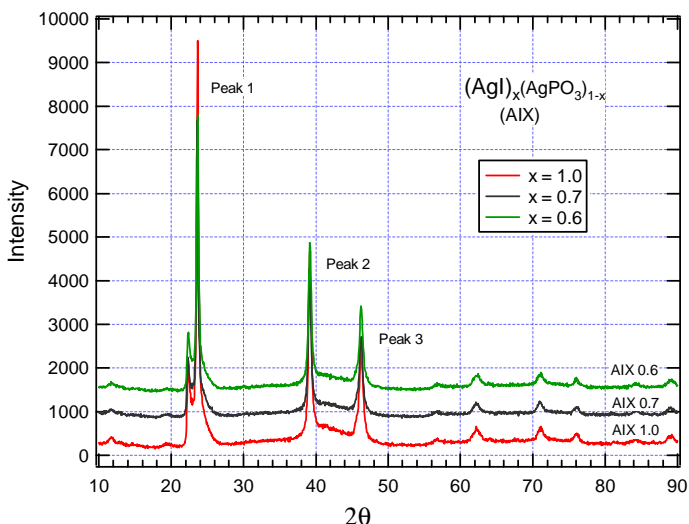

Figure 1. X-ray diffraction patterns of $(AgI)_x(AgPO_3)_{1-x}$ with three different composition (x) : AgI (x = 1.0), $(AgI)_{0.7}(AgPO_3)_{0.3}$ (x =0.7) and $(AgI)_{0.6}(AgPO_3)_{0.4}$ (x = 0.6) at room temperature.

Figure 1 shows the X-ray diffraction patterns with three different composition x, (x =1.0 (pure AgI), 0.7 and 0.6) at room temperature for quenched samples in the system $(AgI)_x(AgPO_3)_{1-x}$. There are Bragg scattering peaks superimposed on the diffuse glass scattering pattern in the superionic glass indicating that the sample is a mixture of $(AgI)_x(AgPO_3)_{1-x}$ glass (x=0.7 and 0.6) and a crystalline precipitate of AgI.

Figure 2 shows first, second and third Bragg's peaks of the diffraction patterns (dot curves) and the results of Gaussian fitting Analysis (solid curves) of pure AgI (AIX 1.0) and composite superionic glass of $(AgI)_x$ $(AgPO_3)_{1-x}$ for both raw data. Compared with the diffraction pattern of AgI, it can be seen that the 2θ peak of AIX 0.6 and 0.7 were shifted to the lower value of 2θ.
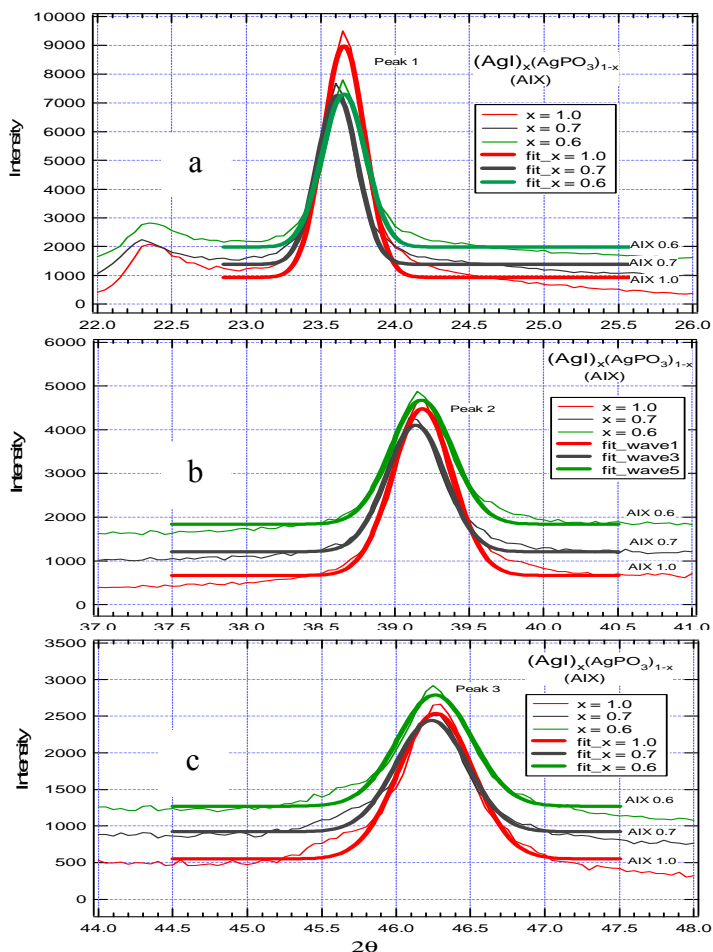
Figure 2. Fitting analysis to the Bragg peaks of $(AgI)_x(AgPO_3)_{1-x}$, for three different x (x = 1.0, 0.7, and 0.6), a) peak 1, b) peak 2 and c) peak 3 by using Gaussian Fitting.

The results of the fitting analysis to the Bragg peaks in $(AgI)_x(AgPO_3)_{1-x}$, at three different values of x (x =1.0, 0.7 and 0.6) and at three different peaks (peaks 1, 2 and 3) respectively are listed in Table 1 and 2. With decreasing composition, in general the peak shifts to the lower angle respectively. The change is caused by rapid quenching of the AgI crystalline in the glass matrix. The composite of $(AgI)_x(AgPO_3)_{1-x}$, where AgI material inhibits more than the solubility limit contains AgI crystal. The data of the fitting analysis to the Bragg peak in $(AgI)_x(AgPO_3)_{1-x}$ at three different composition x (x = 1.0, 0.7 and 0.6) and at three different peaks (peaks 1, 2 and 3) are listed in Table 1 and Figure 2, respectively.

Table 1 shows the data of Bragg reflections which demonstrates that for the material of AIX07 and AIX06, the values of 2θ angle and FWHM for the Bragg reflections on the planes (111), (220) and (311) have decreased in comparison to the AIX1.0 (i.e. pure AgI). These changes are caused by the quenching process as well as the presence AgI crystalline that exists within the glass matrix at a concentration which is above the solubility limit.

Table 1. Bragg angles (θ), HKL and FWHM data of superionic glass $(AgI)_x(AgPO_3)_{1-x}$ (AIX) with various composition x = 0.6 and 0.7 using Gaussian Fitting Analysis.

Material	Peak	HKL	2θ	θ	FWHM (β)	FWHM (radiant)
AIX 1.0	Peak 1	(111)	23.656(4)	11.828(4)	0.200(6)	0.0034(6)
	Peak 2	(220)	39.185(5)	19.593(5)	0.288(7)	0.0047(7)
	Peak 3	(311)	46.267(7)	23.134(7)	0.360(1)	0.0058(1)
AIX 0.7	Peak 1	(111)	23.654(4)	11.806(4)	0.192(6)	0.0033(6)
	Peak 2	(220)	39.140(4)	19.570(4)	0.280(7)	0.0046(7)
	Peak 3	(311)	46.238(6)	23.119(6)	0.341(9)	0.0055(9)
AIX 0.6	Peak 1	(111)	23.652(4)	11.827(4)	0.208(7)	0.0035(7)
	Peak 2	(220)	39.178(5)	19.589(4)	0.295(5)	0.0049(5)
	Peak 3	(311)	46.262(6)	23.131(6)	0.350(1)	0.0056(1)

Table 2. Data of βcosθ and Sinθ on $(AgI)_x(AgPO_3)_{1-x}$ at x = 07, (AIX07) and x = 0.6 (AIX06) to calculate partical size and microstrain.

Table 2. Data analysis of crystal size (D) and microstrain (η) of superionic glass $(AgI)_x(AgPO_3)_{1-x}$ (AIX) with various composition using Gaussian Fitting Analysis.

Materials	Peak	βcos θ	Sinθ	D(Å)	Strain (η)
AIX 1.0 (Pure AgI)	Peak 1	0.0033	0.2050	1260	5.15×10^{-3}
	Peak 2	0.0044	0.3353		
	Peak 3	0.0053	0.3929		
AIX 0.7	Peak 1	0.0032	0.2046	1155	4.9×10^{-3}
	Peak 2	0.0043	0.3350		
	Peak 3	0.0051	0.3926		
AIX 0.6	Peak 1	0.0034	0.2050	900	4.55×10^{-3}
	Peak 2	0.0046	0.3352		
	Peak 3	0.0051	0.3928		

The lattice strain of the γ-AgI crystals in the matrix was estimated through the Hall's analysis using more than two X-ray diffraction peaks [3]. Hall's equation is expressed as :

$$B \cos \theta = \frac{0.94\lambda}{D} + 2\eta \sin \theta \tag{1}$$

Where B is the half-width of a given diffraction peak, λ is the wavelength of X-ray used, η is a measure of the lattice strain, θ is the Bragg angles and D is the crystallite size. Figure 3. shows the relation between $B\cos\theta$ and $\sin\theta$ for (110) and (220) diffraction peaks of γ-AgI in the $(AgI)_x(AgPO_3)_{1-x}$, on x = 1.0, 0.7 and 0.6 composites glass at 27°C.
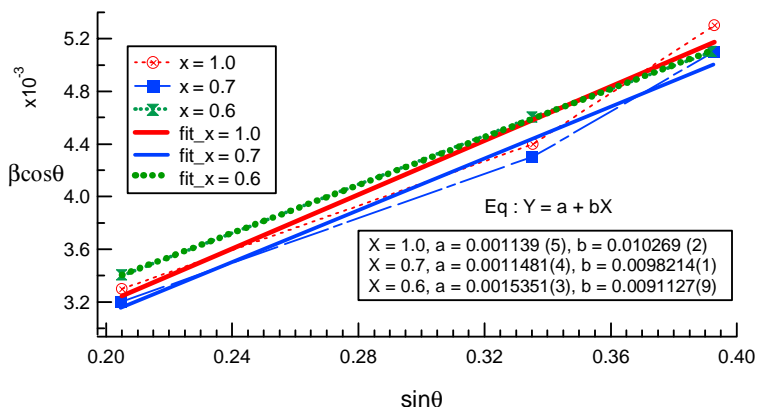

Figure 3. Hall's plots for diffraction Bragg peaks of $(AgI)_x(AgPO_3)_{1-x}$, composites at three different x (x = 1.0 , 0.7, and 0.6), at room temperature.

The values of lattice strain, η in Eq. (1), are obtained from the slopes of the plots. It is apparent that γ-AgI in the composites at 27°C has larger lattice strain compared to the pure α-AgI crystal at room temperature. Such a large lattice strain of frozen α-AgI at 27 $^{\circ}$C is caused by stress at the interface between the AgI crystal and glass matrix during rapid quenching. The surrounding glass matrix suppresses the transformation of γ-AgI to the β-AgI phase, because β-AgI phase is larger than the γ-AgI phase. The crystallite size of γ-AgI in the composite is estimated from the calculation of Hall's plots, i.e equation (1)

The lattice strain, η value is large on pure γ-AgI and decrease with increasing value of x. η value are 4.55 x 10^{-3} (x = 0.6 (AIX 0.6)), 4.9 x 10^{-3} (x = 0.7 (AIX 0.7)) and 5.15 x 10^{-3} (x = 1.0 (AIX 1.0), pure γ-AgI), respectively. While crystal size, D value is large about 1260 Å on pure γ-AgI and decrease with increasing of x. AIX 0.7 = 1155 Å and AIX 0.6 = 900 Å respectively.

CONCLUSION

We have investigated the dependence of composition (i.e x value) on micro strain and particle size of superionic composite glass. The superionic composite glass $(AgI)_x(AgPO_3)_{1-x}$ at $x = 0.7$ and 0.6 was prepared by solid solution reaction and synthezised by melt rapid quenching method. The superionic composite are polycrystalline of γ-AgI phase in face centre cubic, (FCC). The crystalline quality of superionic composite significantly depends on the x composition. The microstrain (η) of the pure AgI ($x =1.0$), $x= 0.7$ and $x = 0.6$ are $5.15 \times 10^{-3}(2)$, 4.9×10^{-3} (1) and 4.55×10^{-3} respectively. While the particle size (D) are 1260 Å, 1155 Å and 900 Å respectively. It is concluded that the solidification process of the melt of AgI into glass matrix $AgPO_3$ decreases the crystal size, due to decreasing the microstrain.

ACKNOWLEDGMENTS

REFERENCES

1. M.F. COLLINS and E. KARTINI, *Solid State Ionic*, **1**, 157 (2003).

2. A. PURWANTO, E. KARTINI, T. KAMIYAMA, A. HOSHIKAWA, S. HARJO, M.F. COLLINS and S. PURNAMA, *Solid State ionics*, **171**, 113 (2004).

3. T. SAKUMA, Y. NAKAMURA, M. HIROTA, A. MURAKAMI, and Y. ISHII, *Solid State Ionics*, **295**, 127 (2000).

4. E. KARTINI and M.F. COLLINS, *Physic B*, **276-278**, 476 (2000).

5. E. KARTINI and M.F. COLLINS, *Physic B,* **276-278**, 467 (2000).

6. T. SUTOMU MINAMI, TOSHIHARU SAITO, and MASAHIRO TATSUMISAGO, *Solid State Ionics*, **86-88**, 415 (1996).

7. M. TATSUMISAGO, Y. SHINKUMA, T. SAITO, and T. MINAMI, *Solid State Ionic,* **50**, 273 (1992).

8. M. TATSUMISAGO, A. TANIGUCHI and T. MINAMI, *J. Am. Ceram.Sos.,* **76**, 235 (1993).

9. T. SAITO, M. TATSUMISAGO, N. TORATA and T. MINAMI, *Solid State Ionic*, **79**, 279 (1995).

10. H.P. KLUG and L.E. ALEXANDER, "X-ray Diffraction Prosedures", 2nd ed, John Willey and Sons, New York (1973).

11. T. SAITO, N. TORATA, M.TATSUMISAGO and T.MINAMI, *J. Physic Chemistry*, **99**, 10691 (1995).